

First Search for Heavy Neutral Leptons with IceCube DeepCore

Dissertation
zur Erlangung des akademischen Grades
doctor rerum naturalium
(Dr. rer. nat.)

im Fach: Physik
Spezialisierung: Experimentalphysik

eingereicht an der
Mathematisch-Naturwissenschaftlichen Fakultät
der Humboldt-Universität zu Berlin

von
Leander Fischer M. Sc.
geboren am 24. Oktober 1992
in Heidelberg

Präsidentin der Humboldt-Universität zu Berlin
Prof. Dr. Julia von Blumenthal

Dekanin der Mathematisch-Naturwissenschaftlichen Fakultät
Prof. Dr. Caren Tischendorf

Copyright Notice

This book is released into the public domain using the CC-BY-4.0 code.

To view a copy of the CC-BY-4.0 code, visit:

<https://creativecommons.org/licenses/by/4.0/>

Colophon

This document was typeset with the help of KOMA-Script and L^AT_EX using the open-source kaobook template class.

The source code of this thesis is available at:

https://github.com/LeanderFischer/phd_thesis

Abstract

In icecube, we have many neutrinos, select some very high energy ones, spend 1 year with them to group them in three flavour categories. I guess we will learn something about where they came from by doing this. Pretty normal stuff, not at all racist.

Zusammenfassung

Im IceCube haben wir viele Neutrinos, von denen wir einige mit sehr hoher Energie auswählen, verbringen 1 Jahr mit ihnen, um sie in drei Geschmackskategorien einzuteilen. Ich vermute, dass wir auf diese Weise etwas darüber erfahren, woher sie kommen. Ziemlich normales Zeug, ganz und gar nicht rassistisch.

Contents

Abstract	iii
Zusammenfassung	v
Contents	vii
1 Neutrinos in IceCube	1
1.1 IceCube Neutrino Observatory	1
1.1.1 Detector	1
1.1.2 The Digital Optical Module (DOM)	3
1.1.3 Trigger and Data Acquisition	5
1.2 Detection of Neutrinos in IceCube	6
1.2.1 Particle propagation in-ice	6
Leptons	6
Hadrons	8
1.2.2 Cherenkov effect	8
1.2.3 Event Signatures	8
1.3 Optical Properties of the South Pole ice	8
APPENDIX	11
Figures	13
Tables	15

1

Neutrinos in IceCube

The birth of neutrino astronomy has led to the development of specific neutrino telescopes designed to explore the cosmos using these elusive particles. This chapter introduces the IceCube Neutrino Observatory, a neutrino detector whose data forms the basis of the analysis presented in this thesis. Later sections will

1.1 IceCube Neutrino Observatory

As described in ??, the detection of high-energy neutrinos requires a large detector due to their small interaction cross-section. When these neutrinos interact, they produce Cherenkov photons which are produced due to the passage of charged daughter particles (see 1.2.2). Therefore, the detector must be transparent to these photons. Such a large detector volume can be acquired by using natural resources such as large bodies of water or ice; by deploying photosensors underneath to create a sufficiently sized detector.

This concept was first introduced in 1960 [Markov:1960vja]. The groundwork for implementing such a detector began with water-based experiments like DUMAND [PhysRevD.42.3613], which was planned to be deployed in the sea near the main island of Hawaii and another detector with a similar design Lake Baikal [BELOLAPTIKOV1997263]. First ever large-scale neutrino telescope built was predecessor of IceCube experiment called AMANDA [ANDRES20001] at the geographic South Pole. A few hundred optical modules were dropped under the ice sheet of this dry continent between the depth of 1.5 to 2 km. Needless to say, the IceCube detector, the largest neutrino telescope in the world today, benefitted greatly in terms of design and performance from all the research and development work that was done with AMANDA. There also exists a large volume water-based neutrino telescope in the Northern Hemisphere called ANTARES[AGERON20111], and its successor KM3NeT[MARGIOTTA201483], located in the Mediterranean Sea.

The following subsections will discuss various detector and hardware components of the IceCube detector. Additionally, the last section will cover the optical properties of the South Pole ice, as these properties strongly affect the analysis observable and therefore influence the flavor measurements presented in this thesis.

1.1.1 Detector

1.1	IceCube Neutrino Observatory	1
1.1.1	Detector	1
1.1.2	The Digital Optical Module (DOM)	3
1.1.3	Trigger and Data Acquisition	5
1.2	Detection of Neutrinos in IceCube	6
1.2.1	Particle propagation in-ice	6
1.2.2	Cherenkov effect	8
1.2.3	Event Signatures	8
1.3	Optical Properties of the South Pole ice	8

Markov:1960vja

PhysRevD.42.3613

BELOLAPTIKOV1997263

ANDRES20001

AGERON20111

MARGIOTTA201483

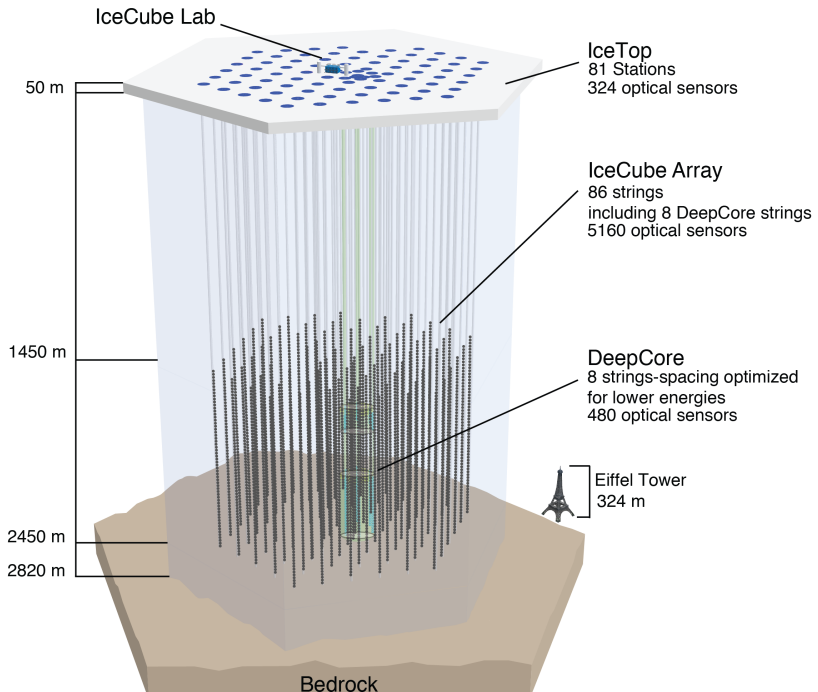


Figure 1.1: A schematic overview of the IceCube detector and its components [Aartsen_2017]

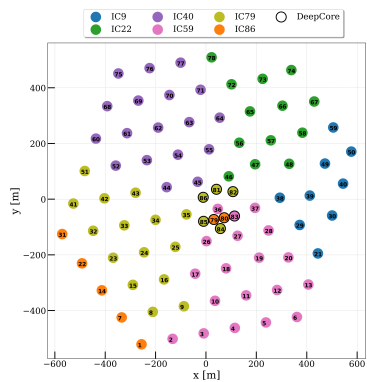


Figure 1.2: Top view of the location of each *in-ice* strings of IceCube. Colour represents set of strings deployed in each seasons as described in Table 1.1. Note: IceTop Stations are not shown here.

Aartsen_2017

string in IceCube

An arrangement of DOMs attached on a twisted copper wire cable makes the so-called *string* in IceCube.

deepcoredesign

Aartsen_2019_oscillations

Abbasi_2022

The IceCube Neutrino Observatory is located at Amundsen-Scott South Pole Station at the geographic South Pole. It comprises a cubic kilometer of instrumented ice, equipped with 5,160 digital optical modules referred as *DOMs* from here-on (see 1.1.2), buried deep in the ice and 81 *IceTop* Stations on the surface of the ice, making itself the largest Neutrino Observatory in the world [Aartsen_2017]. A schematic of the detector layout is shown in Figure 1.1. Four main components of the detector are *in-ice array*, *DeepCore* (*inner extension of in-ice array*), *IceTop* and *IceCube Lab*.

The Main *in-ice* array consists of 78 strings, each consisting of 60 DOMs, spaced vertically at a distance of 17 m between the depth of 1450 m to 2450 m under the ice sheet of Antarctica. Horizontal spacing between each of these strings is 125 m.

DeepCore comprises inner 8 strings (see Figure 1.2) of the main *in-ice* array, placed more closely together with horizontal string distance of 70 m and vertical DOM distance of 7 m [deepcoredesign] between 1750 m to 2450 m depth. There's a region between depth of 1850 m to 2100 m, with no DOMs attached to the string as this region is the so-called *dust layer* (see section 1.3), where optical scattering and absorption is quite high and thus is not efficient to make reliable physics measurements. The Photomultipliers used in DOMs attached on these 7 strings also have higher Quantum Efficiency, which reduces the energy threshold to 10 GeV. Although, IceCube's main goal is to detect astrophysical neutrinos, current topics of research spans much broader range (e.g fundamental properties of the neutrinos, such as oscillations [Aartsen_2019_oscillations], Physics beyond Standard Model searches such as Dark Matter [Abbasi_2022] etc).

IceTop is the surface detector array of the IceCube detector, primarily designed to detect Cosmic-ray airshowers and to be used as a

Season	Configuration	Strings	IceTop Stations
2004-05	IC1	1	4
2005-06	IC9	9	16
2006-07	IC22	22	26
2007-08	IC40	40	40
2008-09	IC59	59	59
2009-10	IC79	79	73
2010-11	IC86	86	81

Table 1.1: IceCube detector components deployed in each season (cumulative). Each configuration is represented as ICXX where IC stands for IceCube and XX stands for number of total *in-ice* strings at the end of that season

veto layer for downgoing muons produced in these airshowers [ABBASI2013188]. It consists of 81 *stations* each having 2 tanks filled with clear ice (162 tanks in total). Each of these 162 tanks have 2 DOMs, similar to the ones deployed in *in-ice* array, which makes it easier for both arrays to have a similar trigger and data acquistion system.

IceCube Lab(ICL) serves as the central operations' hub for the experiment, providing a crucial support for data acquisition and filtering. All the string cables connected to the aforementioned detctior components are routed up to the ICL, from where triggered data is sent back to the northern hemispher via a satellite. Various other operations such as mainting the detector operations etc are also maintained from this building.

For the work presented in this thesis, neither *deepcore* nor *IceTop* data is used.

The construction of the detector started taking place in 2005 and lasted for 7 Antarctic summer seasons till 2011 December. In each season, parts of the current day Hexagonal detector were deployed, as shown in Figure 1.2 and numbers detailed in Table 1.1. A hot water drill was used to unfreeze the ice upto 2.5 km depth and 60 cm diameter into which these strings were then deployed (see Figure 1.3). The geometry of the detctior, i.e The *xy*-coordinates of the string were calculated from the drill tower position, surveyed during the deployment. Assuming the string was vertical, these coordinates were applied at all depths, with deviations of less than 1 m (later validated using the flasher data, see 1.1.3). Depths of the lowest DOM were determined from pressure readings, corrected for water compressibility and ambient air pressure, with vertical DOM spacings measured via laser ranger. All depths were converted to z-coordinates in the IceCube coordinate system .

1.1.2 The Digital Optical Module (DOM)

The Digital Optical Module (DOM) is a crucial component of the IceCube Neutrino Observatory, functioning as the heart of the detector. Each DOM is responsible for collecting the faint light signals produced by neutrino interactions in the Antarctic ice, amplifying these signals, and transmitting the data to the IceCube Lab [Aartsen_2017]. From there, the data is relayed to the Northern Hemisphere via a satellite for further analysis.

Inside each DOM, a 10-inch Photo Multiplier Tube (PMT) is positioned at the bottom, accompanied by essential circuitry for power conversion, data acquisition, calibration, control, and data transfer. Individual components

ABBASI2013188

IceCube coordinates system

The IceCube coordinate system's origin is at 46500'E, 52200'N, 883.9 m elevation, which is quite close to centre of the *in-ice* array. The y-axis points Grid North (toward Greenwich, UK), the x-axis points Grid East (90 degrees clockwise from North), and the z-axis points "up", forming a right-handed coordinate system.

Maybe draw a small schematic of coordinate system here next to the side note?

of a DOM are as shown in Figure 1.4, functions of each of which is explained briefly below.

Glass Vessel Properties : The glass vessel of the DOM is engineered to withstand the extreme pressures found in the deep Antarctic ice. This includes the constant long-term pressure of about 250 bar and the temporary pressure spikes of up to 690 bar experienced during the refreezing process after deployment using a hot water drill. The vessel is composed of two 0.5-inch thick hollow glass hemispheres, which are joined together with optical glue. This design not only provides a robust and hermetic seal to protect the internal electronics but also maintains the optical clarity necessary for the PMT to function effectively. The glass material is chosen for its strength, transparency, and resistance to the harsh conditions in the ice.

PMT : The PMT within the DOM is a 10-inch diameter tube that utilizes a box-and-line dynode chain with 10 stages to amplify the faint light signals detected in the ice. The PMTs used in standard in-ice DOMs have a quantum efficiency peaking at 25% whereas, DeepCore DOMs, designed to detect lower energy neutrinos, feature PMTs with a higher peak quantum efficiency of 34% near the 390 nm wavelength. These PMTs are operated at a gain of 10^7 .

Gel : A high strength, silicon gel is used between the photocathode area and the glass vessel to provide optical coupling and strong mechanical support to the DOM system. This gel has a high optical clarity, with 97% transmission at 400 nm. It shows no signs of deterioration even after a decade, ensuring reliable performance.

Magnetic Shield : The ambient magnetic field at the South Pole, measuring around 550 milligauss (mG), angled 17 degrees from vertical, can significantly affect the performance of the PMT. This includes reducing collection efficiency by 5-10% and causing gain variations of up to 20%, depending on the PMT's azimuthal orientation. To mitigate these effects, a mu-metal cage is installed around the PMT bulb, extending up to its neck. This cage is constructed from a mesh of 1 mm diameter wires with a spacing of 66 mm. Although this mesh blocks about 4% of the incident light, it substantially reduces the adverse impacts of the magnetic field, ensuring more consistent and reliable performance of the PMT.

PMT Base and High Voltage Boards : The high voltage board includes a Digital to Analog Converter (DAC) and an Analog to Digital Converter (ADC) for precise control and monitoring of the voltages supplied to the PMT. The high voltage generator on this board provides the necessary power, which is then regulated and distributed by the voltage divider circuits on the PMT base board. These circuits are specifically designed for low power consumption, ensuring efficient and stable operation of the PMT.

Main Board : The main board serves as the central processing unit (CPU) of the DOM, managing and coordinating all other electronic components. It digitizes the waveforms detected by the PMT, providing a digital representation of the light signals for further analysis. The main board also temporarily stores data, calibrates the internal clock, and exchanges local coincidence information with neighboring DOMs (see 1.1.3). It communicates directly with the Data Acquisition (DAQ) system, ensuring the seamless transfer

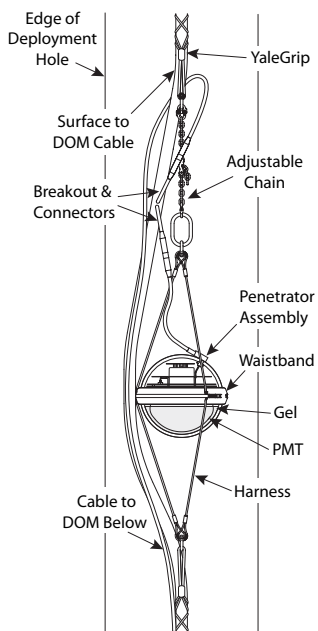


Figure 1.3: A schematic of DOM CableAssembly being deployed in a water hole, created by hot water drill [Aartsen_2017].

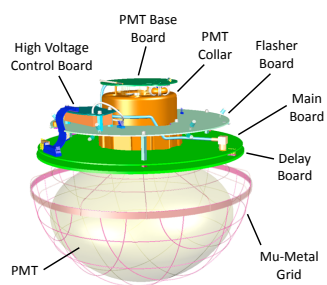


Figure 1.4: A schematic of the DOM, showing its main components [Aartsen_2017].

of data to the IceCube Lab. Additionally, the main board hosts an adjustable low-intensity optical source, which is used to calibrate the PMT's gain and timing, ensuring consistent and accurate performance.

Flasher Board : Flasher board contains 12 LEDs each having specified output wavelength of $405 \pm 5\text{nm}$, which generates lights *in situ* to make various calibration related measurements. In addition, this board can verify timing responses (useful for many, including analysis presented in this thesis, reconstruction processes). Additionally, to measure *the optical properties* of the South Pole Ice (see section 1.3) and locations of the DOMs in ice.

1.1.3 Trigger and Data Acquisition

Ever Since the initial deployment of the first string, the detector has been consistently gathering data, maintaining an average uptime of nearly 99% [Abbasi_2009]. *The photocathode* of the PMT of a DOM, captures a photon which then generates *photoelectrons* which are accelerated through the series of 10 dynodes to generate measurable *photocurrent*. This current is integrated over a time to obtain collected charge in units of *photoelectrons or PEs*, through which *photovoltage* is produced at the mainboard, over time, known as *waveform*. These waveforms are then digitized to acquire and relay the data to the Northern Hemisphere.

Abbasi_2009

Depending on how many photons hit the PMT, these waveforms can have different amplitudes ranging from 1mV upto the linearity limit of the PMT (2 V) in time range of 12-1500 ns. The In Order to access this rather broad dynamic range, the digitiser used, Analog Transient Waveform Digitiser (ATWD) have three channels to amplify the waveform by factor of 0.25, 2 and 16. Moreover, 2 sets of ATWD are used that can operate alternatively in order to reduce the deadtime. ATWD can digitize voltage within duration of 427 ns, a window sufficient to reconstruct light produced within 10s of m around a given DOM. Naturally, some photons produced in energetic interactions may travel larger distances, producing faint but detectable waveforms. To amplify and digitize these waveforms, a fast Analog to Digital Converter (fADC) is also used, together ATWD+fADC is reffered as a *DOMLaunch*.

The aforementioned digitization only happens if the voltage threshold of the onboard discriminator is met, which is kept at voltage equivalent to a PE of 0.25, or in other words, a DOM is *hit*. If at least two neighbouring DOMs, on the same string produces individual *hits* within $1\text{ }\mu\text{s}$ called *Hard Local Coincidence(HLC)*, the full *DOMLaunch* is transmitted to the surface. Otherwise, only the timestamp and minimal amplitude/charge information is sent known as *Soft Local Coincidence(SLC)*. The HLC condition helps reduce false triggers from PMT dark noise, which is independent across DOMs. *The Data Acquisition System (DAQ)* processes further uses these HLC hits to look for temporal coincidences. Most commonly used trigger in IceCube is the so-called *The Single Multiplicity Trigger (SMT-8)*, that requires eight or more HLC hits within $5\text{ }\mu\text{s}$ timewindow. If and when SMT8 trigger conditions are met, all launches (HLC and SLC) are combined into what is called an *event*.

Various algorithms are used to make an estimate of event properties such as direction, deposited energy, morphology etc. The South Pole has limited computational resources, so only simple first guess algorithms can be used there called *online filters*. Processed data is transmitted to the Northern Hemisphere. After this, more sophisticated reconstruction algorithms are applied to reduce and tailor the data as per Physics analysis goal.

cite simulation/reco chapter here

1.2 Detection of Neutrinos in IceCube

As described in ??, regardless of the type of neutrino interaction (NC or CC), a variety of secondary particles are generated. In the case of a CC interaction, an accompanying charged lepton absorbs some energy, which can then undergo further decay or interact within the ice volume, leading to the production of more particles. Moreover, secondary particles, regardless of the interaction type, may also include hadrons, which are not always charged. This can, in turn, reduce the amount of *visible* light in the detector. In this section, propagation of these leptons and hadrons in ice shall be explained in brief, followed by Cherenkov effect, a phenomenon by which IceCube DOMs observes these photons from the neutrino interactions. Lastly, various morphologies of these interactions will be discussed in the context of IceCube and similar detectors.

1.2.1 Particle propagation in-ice

When a charged particle moves through a medium like ice, it loses energy due to interactions with the medium's particles. This energy loss is characterized by the quantity $\frac{dE}{dx}$, where dE represents the energy lost and dx the area of the medium traversed, typically measured in g/cm². Four primary processes contribute to the energy loss profile of a particle in such a medium: continuous ionization losses and radiative losses due to bremsstrahlung, pair production, and photonuclear interactions. *Ionization* occurs when the particle collides with shell electrons of the atoms in the medium, causing a continuous energy loss that scales logarithmically with the particle's energy [PDG_2024].

PDG_2024

Radiative losses, such as *bremsstrahlung*, occur when the charged particle is deflected through Coulomb scattering off a target atom, while *pair production* involves the creation of an electron-positron pair by an emitted photon. *Photonuclear interactions* occur when a photon emitted by the particle disintegrates an atomic nucleus. These radiative losses are stochastic and scale roughly linearly with the particle's energy, with the radiation length X_0 defining the distance over which the particle's energy decreases to $\frac{1}{e}$ of its initial value [PDG_2024]. The overall energy loss can be expressed as $-\frac{dE}{dx} = a(E) + b(E)E$, where $a(E)$ represents ionization losses and $b(E)$ encompasses all radiative losses.

Leptons

To determine a neutrino's flavor, it's important to understand the energy losses of the charged lepton created in a CC-interaction. The radiation

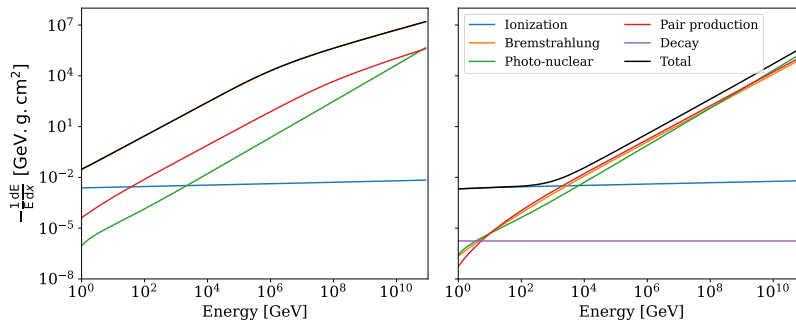


Figure 1.5: The average energy loss rate per energy, for electrons (left) and muons (right) in ice showing the contributions from ionization, bremsstrahlung, photonuclear interactions, and pair production. Note that from [152].

length varies depending on the lepton's mass, influencing emitted radiation and aiding in lepton identification. For leptons with $\beta\gamma \gg 1$, this ionization loss can be approximated as constant, with a value of $\langle \frac{dE}{dx} \rangle_{\text{ion}} \approx 2 \text{ MeV}/(\text{g/cm}^2)$ [Perkins]. In ice, this corresponds to a continuous energy loss of approximately 180 MeV per meter. However, at energies exceeding 1 TeV, which are pertinent to IceCube analyses, radiative losses become dominant, and ionization losses become negligible, as shown in the Figure 1.5 [MMC_paper].

Perkins

MMC_paper

For electrons, we mainly consider radiative losses, especially bremsstrahlung. Electrons are stable and do not decay. Photons from bremsstrahlung then create additional $e^+ e^-$ pairs which can create more photons and so on, resulting in a cascade of particles until the energies of electrons and positrons fall below the critical level. This behavior can be described by a gamma distribution, regardless of what the initiating particle is ($e^+ e^-$ or γ) [PDG_2024]. The rate of energy loss over distance can be calculated using the equation:

$$\frac{dE}{dt} = E_0 b \left(\frac{(bt)^{a-1} e^{-bt}}{\Gamma(a)} \right) \quad (1.1)$$

where t represents the distance along the cascade in units of radiation length, and E_0 is the initial energy of the injected particle. For an electromagnetic cascade induced by an electron, the parameters are $a = 2.02 + 0.63 \log(E_0/\text{GeV})$ and $b = 0.63$ (determined using GEANT4 simulations [shower_profile]). The distance to the shower maximum, t_{\max} , which is given as $\frac{a-1}{b}$ characterizes the size of electromagnetic cascades, indicating that they grow logarithmically in size with energy and have a characteristic size of several meters. This justifies the common approximation that light is emitted from a single point, a useful assumption for simulation and event reconstruction purposes.

shower_profile

reference reco chapter here

At very high energies ($> 10 \text{ PeV}$), the Landau-Pomeranchuk-Migdal (LPM) effect becomes significant, causing suppression of bremsstrahlung and pair production cross sections [LPM1, LPM2, LPM3]. This suppression occurs due to destructive interference between multiple scattering centers, leading to elongated and irregular shower profiles.

LPM1, LPM2, LPM3

Additionally, if the lepton is unstable, it may decay. The decay time in the laboratory frame is dilated, as described by special relativity, and the propagation distance before decay, known as the decay length λ_{dec} , is given by $\lambda_{\text{dec}} = c\beta\gamma\tau$. Here, c is the speed of light, β is the lepton's velocity as a fraction of the speed of light, γ is the Lorentz factor, and τ is the lepton's lifetime in its rest frame ($\tau_\mu = 2.2 \times 10^{-6} \text{ s}$ and

$\tau_\tau = 290.3 \times 10^{-15}$ s [PDG_2024]). In the context of IceCube, secondary leptons travel at nearly the speed of light, simplifying β to approximately 1. Thus, the decay length can be rewritten as $\lambda_{\text{dec}} = \frac{E\tau}{mc}$, where E is the lepton's energy and m its mass. The decay length indicates the distance at which the lepton's survival probability drops to $\frac{1}{e} \approx 36.8\%$, following the exponential decay law $p(L) = \exp(-L/\lambda_{\text{dec}})$. For instance, a 1 TeV muon has a decay length of around 6242 km, while a tau lepton of the same energy has a much shorter decay length of approximately 4.9 cm, reflecting the significant mass difference between the muon and tau ($m_\mu = 105.67 \text{ MeV}/c^2$, $m_\tau = 1776.93 \text{ MeV}/c^2$) [PDG_2024].

Hadrons

1.2.2 Cherenkov effect

1.2.3 Event Signatures

1.3 Optical Properties of the South Pole ice

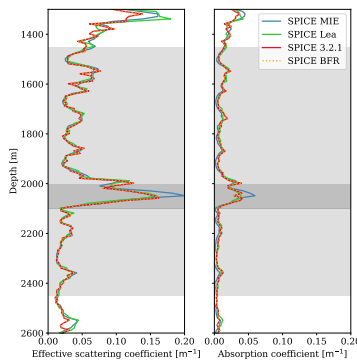


Figure 1.6: Values of effective scattering (left) and absorption (right) coefficients of 400nm photons in South Pole Ice as a function of depth, for four icemodels described in the text. Light grey area shows in-ice array and dark grey region shows the high absorption and scattering region called *the dust layer*.

optical_properties_amanda
dust_logger
spicemie

The ice at the South Pole is a crucial part of the IceCube detector. It acts as both the detection target and the medium through which light propagates. Unlike the DOM hardware, which has been extensively studied in the laboratory, the glacial ice can only be measured in its actual environment, making it more challenging to describe. Understanding and calibrating this medium well is essential for accurate physics measurements as photons produced from particle interactions can get absorbed or scattered from their path, making the inference of the particle interaction points challenging.

In context of Neutrino Detection, The ice at the deep South Pole was initially measured using pulsed in situ light sources (LEDs) at different wavelengths, embedded in the AMANDA array below 1000 m depth[optical_properties_amanda]. Later, during the construction of IceCube, direct measurements of dust concentration in the glacial ice were obtained using a dust logger deployed into some drill holes [dust_logger]. Additionally, the LEDs on the Flasher Board of DOMs are still actively used to calibrate the detector and understand the ice properties [spicemie].

The scattering length (l_s) is the average distance a photon will travel before scattering off of its original directory. In practice, only the effective scattering length ($l_{\text{eff}} = \frac{l_s}{1 - \langle \cos \theta \rangle}$) can be measured, where $\langle \cos \theta \rangle$ is the average deflection angle at each scatter. The absorption length (l_a) is the distance after which a photon's survival probability decreases to $1/e$, indicating how far the information from an event can travel. In the case of absorption, the photon is lost, while for scattering, its direction changes, affecting both the energy and direction reconstruction of the event. Scattering and absorption parameters in *ice models* are averaged over 10-meter-thick layers of ice and are calculated for a wavelength of 400 nm [spicemie]. Light scattering below a depth of about ~1300 m is mainly due to residual air bubbles. As depth increases, dust becomes the main source of scattering, with concentration varying due to climate and volcanic activity. At around 2000 meters, scattering and absorption

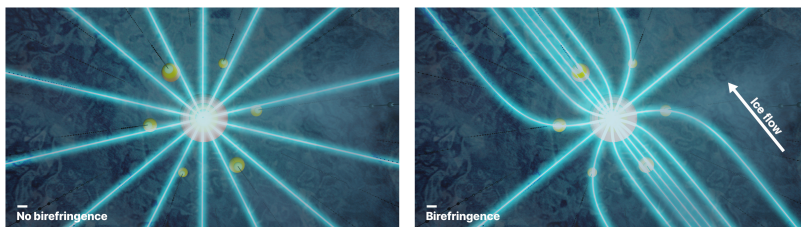


Figure 1.7: The visualisation of deflection due to birefringence. Without it (left panel), light streams out radially from an isotropic source. With this effect however (right panel), rays get deflected towards the flow axis, appearing as though photons are scattered "more" along this axis. The IceCube array around the light source can be seen as well. (Figure taken from [BFR_paper])

significantly increase due to high dust concentration, possibly from a major volcanic eruption in the past, known in IceCube as **the dust layer** [**dustlayer**] (see Figure 1.6). This layer is either omitted or treated more carefully in most analyses as information carried by photons coming and going through this layer is difficult to traceback due to higher scattering coefficient.

The data from the dust logger also revealed that the ice layers are not perfectly horizontal; they are tilted due to the uneven surface of the bedrock [**dust_logger**], the so-called **ice tilt**. Initially, the effect was symmetrically parameterized along an axis (referred to as *the tilt axis*) that is approximately perpendicular to the glacial flow and also dependent on depth (same as the layers used to characterise absorption and scattering lengths described before) [**spicemie**]. As a result, the scattering and absorption coefficients became dependent on the full three-dimensional position in the ice rather than just the depth. A recently developed fully volumetric tilt model now includes a newly discovered tilt component along the flow [**tilt_icrc**].

Another unique property that the South Pole ice exhibits is optical **anisotropy**, a phenomenon affecting photon propagation depending on their direction relative to the "axis of anisotropy," which coincides within $\sim 1^\circ$ with the direction of the ice flow [**spicemie**]. This effect was initially implemented as a modification to the scattering function, the only remaining Mie scattering parameter [**miescattering**], thereby changing the scattering length [**bfr_icrc2013**, **marcel_thesis**]. However, recent detailed studies suggest that this behavior results from diffusion within the polycrystalline ice microstructure, a previously unknown optical effect, now known as Birefringence [**bfr_icrc2019**, **BFR_paper**]. This effect causes the ice crystals to slowly but continuously deflect towards the normal vector of the girdle plane of the crystal orientation fabric (the ice flow axis), as can be seen in Figure 1.7.

In the context of the IceCube Detector, South Pole ice can be divided into two types: bulk ice and hole ice. Bulk ice is the undisturbed part of the ice, consisting of sheets that have formed over hundreds of thousands of years, properties of which are described above. **Hole ice**, on the other hand, is the refrozen column of ice that was melted during the deployment of the DOMs [**holeice_dima_icrc21**]. This effect generally affects the forward acceptance of the IceCube DOMs. If not taken care of, it can lead to errors in directional information, thereby affecting measurements involving zenith angle reconstructions of the incoming neutrino. Over the years, many efforts have been made to understand various optical properties of the South Pole ice, by fitting the LED data in terms of absorption and scattering lengths of a Cherenkov photon in ice, the so-called **South Pole ICE model (SPICE model)**. These icemodels are used in both simulation

dustlayer

tilt_icrc

miescattering

bfr_icrc2013, marcel_thesis

bfr_icrc2019, BFR_paper

holeice_dima_icrc21

and reconstruction of the events, where particles produced in neutrino interactions are propagated (see 1.2.1) based scattering and absorption lengths described by the model. While the base model for the scattering of the photons in-ice is Mie Scattering theory [**miescattering**] (SPICE MIE), with more dust loggers data, evolved more complex models to include, anisotropy (SPICELea), addition of tilt (SPICELea, SPICE 3.2.1), birefringence to explain anisotropy (SPICEBfr) and the latest, SPICE FTP, which includes a 2D tilt correction in addition to birefringence. Figure 1.6 shows absorption and scattering coefficients for different ice models at various depths in the detector. The corresponding scattering and absorption lengths are simply the inverse of the coefficients. It can be seen that the ice below the depth of ~ 1400 m is so clear that light can travel for hundreds of meters before being absorbed. However, the light diffuses quickly, making a point-like source appear nearly isotropic at a distance of around 100 m. Effect of different icemodel corrections (specifically that of anisotropy related corrections) becomes quite relevant to reconstruct tau-neutrino events in IceCube, which is heart of the analysis presented in this thesis.

APPENDIX

List of Figures

1.1	A schematic overview of the IceCube detector and its components [Aartsen_2017]	2
1.2	Top view of the location of each <i>in-ice</i> strings of IceCube. Colour represents set of strings deployed in each seasons as described in Table 1.1. Note: IceTop Stations are not shown here.	2
1.3	A schematic of DOM CableAssembly being deployed in a water hole, created by hot water drill [Aartsen_2017].	4
1.4	A schematic of the DOM, showing its main components [Aartsen_2017].	4
1.5	The average energy loss rate per energy, for electrons (left) and muons (right) in ice showing the contributions from ionization, bremsstrahlung, photonuclear interactions, and pair production. Note that from [152].	7
1.6	Values of effective scattering (left) and absorption (right) coefficents of 400nm photons in South Pole Ice as a function of depth, for four icemodels described in the text. Light grey area shows in-ice array and dark grey region shows the high absorption and scattering region called <i>the dust layer</i>	8
1.7	The visualisation of deflection due to birefringence. Without it (left panel), light streams out radially from an isotropic source. With this effect however (right panel), rays get deflected towards the flow axis, appearing as though photons are scattered "more" along this axis. The IceCube array around the light source can be seen as well. (Figure taken from [BFR_paper])	9

List of Tables

1.1 IceCube detector components deployed in each season (cumulative). Each configuration is represented as <i>ICXX</i> where <i>IC</i> stands for IceCube and <i>XX</i> stands for number of total <i>in-ice</i> strings at the end of that season	3
--	---